ON THE SPACE OF PLANAR BRANCHED POLYMERS WITH FIXED TANGENCY GRAPH

TRISTAN SHIN

UROP+ Final Paper, Summer 2020
Mentor: Vishal Patil
Project suggested by: Vishal Patil

Abstract. Planar branched polymers, as studied by Brydges and Imbrie, are connected sets of n labelled unit disks. We provide analytic descriptions of the subspace of branched polymers with fixed tangency graph. Using this, we compute the volumes of the subspaces whenever the tangency graph is a tree with diameter at most 3 and verify that they occupy a rational fraction of the total space of branched polymers with the same order. Under a natural embedding of the space of branched polymers with fixed tangency graph into Euclidean space, we show that the connected components of the embedding are convex whenever the tree has diameter at most 3. By relating branched polymers to self-avoiding walks, we find that the nth root of an appropriately rescaled version of the volumes converges to a constant. Finally, we examine trees that are impossible as tangency graphs, demonstrating that the set of maximum degrees of the smallest such trees (in a subgraph sense) is precisely $\{3, 4, 5, 6\}$.

1. Introduction

A **branched polymer** of order n in $\mathbb{R}^d$ is a connected set of n labelled unit $(d-1)$-spheres with disjoint interiors, where the sphere labelled as 1 is centered at the origin (Figure 1). Each branched polymer has an underlying **tangency graph** defined as the graph T on n vertices corresponding to the n disks, with edges between vertices with tangent corresponding disks.

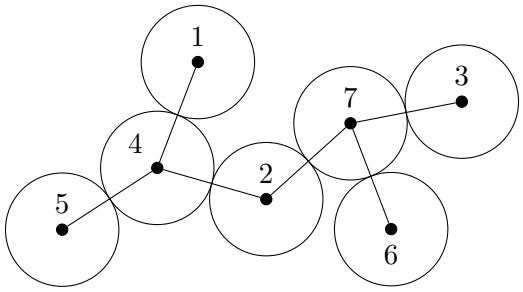

Figure 1. A branched polymer in $\mathbb{R}^2$, also called a planar branched polymer.

Branched polymers are models of objects of the same name in chemistry. The models are typically defined as trees on a lattice, usually $\mathbb{Z}^d$, in a generalization of self-avoiding walks. However, Brydges and Imbrie [1] as well as Kenyon and Winkler [8] displayed several properties of this continuous version of polymers, creating a new mathematical model for these scientific objects.

We can create a natural parametrization of the space of branched polymers of order n, as used by Kenyon and Winkler [8]. First specify a labelled tree that serves as a spanning tree of the

Department of Mathematics, Massachusetts Institute of Technology, Cambridge, MA 02139
E-mail address: shint@mit.edu.
Date: 31 Aug 2020.

tangency graph, then specify $(n-1)$ d-dimensional angles corresponding to the angles of the vectors between centers of tangent spheres. Under such a parametrization, we are able to define the $(n-1)$-dimensional space $B^d(n)$ of branched polymers of order n as defined by Kenyon and Winkler [8]. We are additionally able to consider a notion of volume using these coordinates. This parametrization may be ambiguous for polymers whose tangency graphs contain cycles and hence have multiple spanning trees, but the space of such polymers has volume zero under these coordinates so there is no issue.

In this paper, we restrict our attention to the case $d = 2$ of planar branched polymers. For each tree T, let $\mathrm{BP}(T)$ denote the space of branched polymers with tangency graph T and any labelling of T. Note that $B^2(n)$ is the disjoint union of $\mathrm{BP}(T)$ over all trees T of order n, as well as some sets with volume zero, so the following equation holds:

$$\mathrm{Vol}(B^2(n)) = \sum_T \mathrm{Vol}(\mathrm{BP}(T)).$$

Brydges and Imbrie [1] proved the following key theorem using non-constructive techniques:

Theorem 1.1. *For all $n \in \mathbb{N}$,*

$$\mathrm{Vol}(B^2(n)) = (n-1)! \cdot (2\pi)^{n-1}.$$

Kenyon and Winkler [8] gave an elementary proof of Theorem 1.1 using the following lemma which stemmed from the original proof by Brydges and Imbrie:

Lemma 1.2 (Invariance Lemma)**.** *Consider a generalization of branched polymers in which the $(d-1)$-spheres instead have radii given by some vector $\mathbf{r} = (r_1, \ldots, r_n)$, and let $B^2_{\mathbf{r}}(n)$ be the space of branched polymers of order n with this radius vector. Then $\mathrm{Vol}(B^2_{\mathbf{r}}(n))$ is independent of $\mathbf{r}$.*

The invariance lemma can be interpreted as a statement that as the radius vector changes, volume flows between the different $\mathrm{BP}_{\mathbf{r}}(T)$ (defined similarly to $\mathrm{BP}(T)$ but for arbitrary radius vector) through the boundaries. The boundaries of $\mathrm{BP}_{\mathbf{r}}(T)$ with codimension k correspond to branched polymers whose tangency graph has k cycles and T as a spanning tree. Thus volume can flow out of $\mathrm{BP}_{\mathbf{r}}(T)$ through a codimension-1 boundary piece to $\mathrm{BP}_{\mathbf{r}}(T')$ for a tree T' formed by adding an edge to T and deleting a different edge from the resulting cycle.

In the case of $\mathbf{r} = (1, \ldots, 1)$, Kenyon and Winkler posed the question of determining $\mathrm{Vol}(\mathrm{BP}(T))$ for each T, also asking if they are always rational multiples of $(2\pi)^{n-1}$. As shown in Figure 2, there are two types of branched polymers of order 4, with their volumes being rational multiples of $(2\pi)^3$. The goal of this paper is to investigate this question as well as the structure of $\mathrm{BP}(T)$.

Figure 2. Up to isomorphism, there are two trees on 4 vertices—the path graph and the star graph. The path graph has volume $40\pi^3$ while the star graph has volume $8\pi^3$, so the total volume of $B^2(4)$ is $48\pi^3 = 3! \cdot (2\pi)^3$.

To analyze the space $\mathrm{BP}(T)$, it is helpful to define $\mathrm{BP}_L(T)$ to be the space of branched polymers with tangency graph T and fixed labelling (up to automorphism) of T. Note that all $\mathrm{BP}_L(T)$ are congruent for varying labellings of a fixed T, so it will not matter which labelling we choose. For brevity, let $V_L(T)$ denote the volume of $\mathrm{BP}_L(T)$.

Let $\mathrm{Aut}(T)$ be the automorphism group of T. Then by considering the group action of the symmetric group on the set of labelled trees with n vertices and applying the orbit-stabilizer

theorem, there are $\frac{n!}{|\mathrm{Aut}(T)|}$ labellings of T. But observe that $\mathrm{BP}(T)$ is composed of one copy of $\mathrm{BP}_L(T)$ for each labelling of T, so

$$\mathrm{Vol}(\mathrm{BP}(T)) = \frac{n!}{|\mathrm{Aut}(T)|} \cdot V_L(T).$$

Thus to address the questions about $\mathrm{Vol}(\mathrm{BP}(T))$, it suffices to examine $V_L(T)$.

This paper is split into several sections. In Section 2, we provide a useful way to partition $\mathrm{BP}(T)$ into smaller subspaces and a more concrete definition of coordinates which can be used to parametrize $\mathrm{BP}_L(T)$. Using these coordinates, we create a natural embedding of $\mathrm{BP}_L(T)$ into the hypercube $[0, 2\pi)^{n-1}$. In Section 3, we provide an analytic description of the boundary of $\mathrm{BP}_L(T)$, demonstrating that certain faces of the boundary of the embedding are actually hyperplanes. Using this fact, we compute the volume of $\mathrm{BP}(T)$ whenever $\operatorname{diam} T \leq 3$ and verify that it is a rational multiple of $(2\pi)^{n-1}$. This characterization of the boundary additionally allows us to demonstrate that the embedding of $\mathrm{BP}_L(T)$ is convex whenever $\operatorname{diam} T \leq 3$ but is not when T is the path graph of length at least 4. In Section 4, we prove a result on the order of growth of $V_L(T)$, namely the existence of a connective constant for the sequence of volumes for path graphs, by relating branched polymers to self-avoiding walks. In Section 5, we exhibit some trees T for which $\mathrm{BP}(T)$ has volume zero, demonstrating that the set of maximum degrees of the smallest such trees (in a subgraph sense) is precisely $\{3, 4, 5, 6\}$.

Acknowledgements. The author would like to thank Vishal Patil for providing mentorship, resources, and guidance throughout the project, as well as suggesting the research topic. The author would also like to thank the MIT Department of Mathematics, in particular Slava Gerovitch, David Jerison, and Ankur Moitra, for organizing the UROP+ program through which this research was produced. This research was funded by the John Reed fund as a summer UROP project in the MIT Department of Mathematics.

2. Preliminaries

In this section, we describe a partitioning of $\mathrm{BP}(T)$ into smaller subspaces which will make analyzing the space easier. We then provide a parametrization of polymers with fixed tangency graph.

To do this, we begin by generalizing the notion of a branched polymer by defining a crossing polymer to be the same as a branched polymer but allowing overlapping interiors (Figure 3).

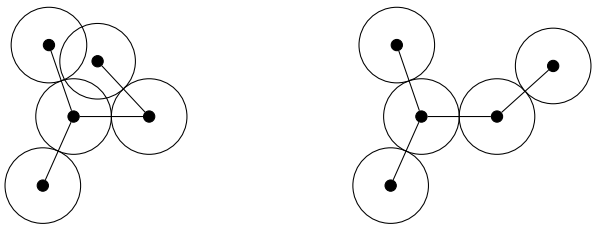

Figure 3. A crossing polymer and branched polymer with the same tangency graph.

In a similar vein to branched polymers, we will let $\mathrm{CP}_L(T)$ be the space of crossing polymers with tangency graph T and fixed labelling (up to automorphism) of T, so that $\mathrm{BP}_L(T)$ is a subspace of $\mathrm{CP}_L(T)$. By constructing a crossing polymer in $\mathrm{CP}_L(T)$ inductively, we have that $\mathrm{CP}_L(T) \cong \mathbb{T}^{n-1}$, the $(n-1)$-dimensional torus.

2.1. **Partitioning** $\mathrm{BP}(T)$ **into smaller subspaces.** The space $\mathrm{BP}(T)$ can be partitioned into subspaces in a useful manner. First, we can divide $\mathrm{BP}(T)$ into $\frac{n!}{|\mathrm{Aut}(T)|}$ congruent subspaces of the form $\mathrm{BP}_L(T)$ as described in Section 1. We can further refine the partition by splitting $\mathrm{BP}_L(T)$ into its connected components.

Here, we say that two branched polymers are in the same connected component if it is possible to rotate the disks while remaining in $\mathrm{BP}(T)$ to get from one to the other (Figure 4). We will see in Section 2.2 that this notion of connected coincides with the standard topological notation of connected when we parametrize $\mathrm{BP}_L(T)$.

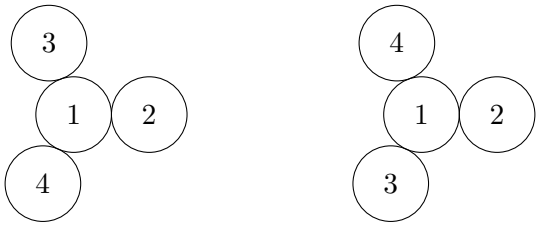

Figure 4. Two branched polymers in $\mathrm{BP}_L(T)$ that are in different connected components, where T is the star graph on 4 vertices.

Based on the possible ways to cyclically permute the disks tangent to a single disk, the total number of connected components of $\mathrm{BP}_L(T)$ is at most

$$\prod_{v \in V(T)} (\deg v - 1)!$$

where the permutations around each vertex v contribute $(\deg v - 1)!$ to the product.

In general, the connected components might be non-congruent (Figure 5). There exist trees where all connected components of $\mathrm{BP}_L(T)$ are congruent though; for example, both connected components of the graph T shown in Figure 4 are congruent.

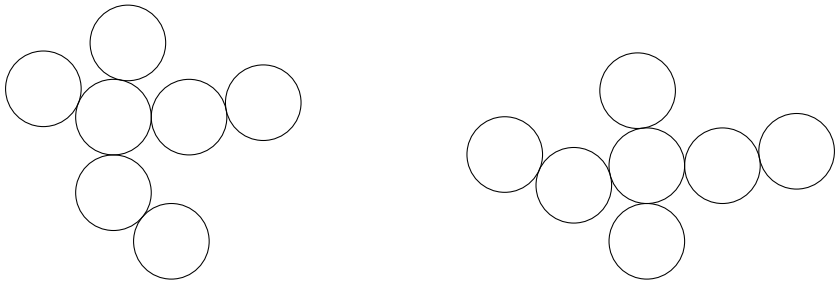

Figure 5. Two elements of $\mathrm{BP}_L(T)$ for the same T in non-congruent connected components.

2.2. **Parametrization.** We describe two parametrizations of the space $\mathrm{CP}_L(T)$ that we will use. In both parametrizations, we assume that the vertex labelled as 1 is a leaf and all parents are labelled smaller than their children when rooting the tree at 1. Furthermore, let O_k for $k = 1, \ldots, n$ denote the center of the disk labelled as k.

The first parametrization, essentially the one given by Kenyon and Winkler, is straightforward and intuitive. For $v = 2, \ldots, n$, let $\hat{\theta}_v$ denote the argument of the vector $\overrightarrow{O_p O_v}$, where p is the parent of v (Figure 6). Then the **argument parametrization** of $\mathrm{CP}_L(T)$ is the parametrization

$(\hat{\theta}_2, \ldots, \hat{\theta}_n) \in \mathbb{T}^{n-1}$. It is also convenient to define $\hat{\theta}_{uv}$ for every edge uv to be the argument of the vector $\overrightarrow{O_u O_v}$. It is straightforward to check that

$$\hat{\theta}_{uv} = \begin{cases} \hat{\theta}_v & \text{if } u < v \\ \hat{\theta}_u - \pi & \text{if } v < u \end{cases}$$

where equality holds modulo 2π (working in the torus). Given these angles $\hat{\theta}_v$ and $\hat{\theta}_{uv}$ taken modulo 2π, we can define the representatives of the angles to be $\theta_v \in [0, 2\pi)$ and $\theta_{uv} \in [0, 2\pi)$ such that $\theta_v \equiv \hat{\theta}_v \pmod{2\pi}$ and similarly with θ_{uv}.

The other parametrization concerns the argument with respect to the parent edge. Let $\hat{\varphi}_2$ denote the counterclockwise angle from the vector $(-1, 0)$ to $\overrightarrow{O_1 O_2}$. For $v = 3, \ldots, n$, let $\hat{\varphi}_v$ denote the counterclockwise angle from $\overrightarrow{O_p O_q}$ to $\overrightarrow{O_p O_v}$, where p is the parent of v and q is the parent of p (Figure 6). Then the **previous edge parametrization** of $\mathrm{CP}_L(T)$ is the parametrization $(\hat{\varphi}_2, \ldots, \hat{\varphi}_n) \in \mathbb{T}^{n-1}$. It is also convenient to define $\hat{\varphi}_{uvw}$ for every path uvw of length 2 to be the counterclockwise angle from $\overrightarrow{O_v O_u}$ to $\overrightarrow{O_v O_w}$. It is straightforward to check that

$$\hat{\varphi}_{uvw} = \begin{cases} \hat{\varphi}_w & \text{if } u < v < w \\ 2\pi - \hat{\varphi}_u & \text{if } w < v < u \\ \hat{\varphi}_w - \hat{\varphi}_u & \text{if } v < u, w \end{cases}$$

where equality holds modulo 2π. Note that $v > u, w$ never holds because this would mean that v has a child (either u or w) with smaller label than itself. We can define φ_v and φ_{uvw} similarly to how we defined θ_v and θ_{uv}. We will later see that $\varphi_v \in (0, 2\pi)$ for all $v > 2$, so we actually have the exact equality:

$$\varphi_{uvw} = \begin{cases} \varphi_w & \text{if } u < v < w \\ 2\pi - \varphi_u & \text{if } w < v < u \\ \varphi_w - \varphi_u & \text{if } v < u, w \text{ and } \varphi_w \geq \varphi_u \\ 2\pi + \varphi_w - \varphi_u & \text{if } v < u, w \text{ and } \varphi_w < \varphi_u \end{cases}$$

Remark 2.1. A small angle chase reveals that $\hat{\varphi}_{uvw} = \hat{\theta}_{vw} - \hat{\theta}_{vu}$, so $\hat{\varphi}_v = \hat{\theta}_v - \hat{\theta}_p + \pi$ for $v \geq 3$. Consequently, the previous edge parametrization leads to the same notion of volume as the argument parametrization and thus as referred to by Kenyon and Winkler [8].

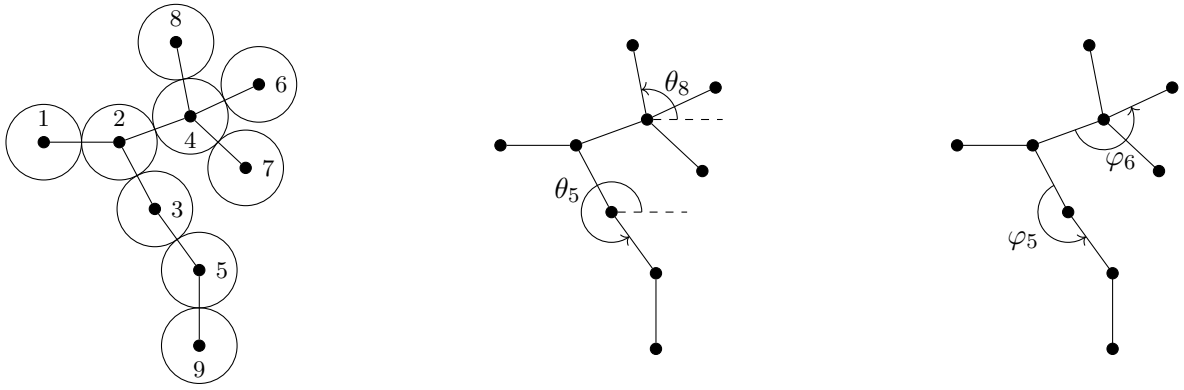

Figure 6. A branched polymer and the two parametrizations (argument parametrization in the middle, previous edge parametrization on the right).

Using the previous edge parametrization, there is a natural volume-preserving map from $\mathrm{CP}_L(T)$ to $[0,2\pi)^{n-1}$ sending $(\hat{\varphi}_2,\dots,\hat{\varphi}_n)$ to $(\varphi_2,\dots,\varphi_n)$. Let $\mathrm{BP}_L^E(T)\subset[0,2\pi)^{n-1}$ be the image of $\mathrm{BP}_L(T)$ under this map into Euclidean space. This embedding of $\mathrm{BP}_L(T)$ is important not only because it preserves volume, but also because it preserves connectivity. That is, each connected component of $\mathrm{BP}_L(T)$ (in the sense of rotation as described above) corresponds precisely with a connected component of $\mathrm{BP}_L^E(T)$ (in the topological sense).

These connected components can very easily be described by the coordinates. If $v_1,\dots,v_{d-1}$ are all of the children of a vertex, then each of the $(d-1)!$ orderings of the numbers $\varphi_{v_1},\dots,\varphi_{v_{d-1}}$ corresponds to a different subset of connected components.

2.3. **Important families of trees.** There are a few important families of trees. We will use P_k to denote the path graph on k vertices and S_a to denote the star graph on $a+1$ vertices (a leaves adjacent to a "center" vertex). We will also use $S_{a,b}$ to denote the graph on $a+b+2$ vertices formed by joining S_a and S_b with an edge between their centers (Figure 7).

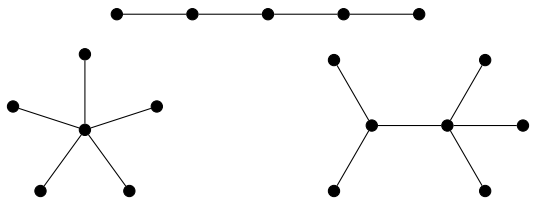

Figure 7. The graphs P_5 (top), S_5 (bottom left), and $S_{2,3}$ (bottom right).

3. The space $\mathrm{BP}_L(T)$

Using the parametrization provided in Section 2, we provide an analytic description of $\mathrm{BP}_L(T)$ as a subspace of $\mathrm{CP}_L(T)$. We then show that boundaries of $\mathrm{BP}_L^E(T)$ corresponding to paths in T of length at most 3 are hyperplanes. This allows us to compute $\mathrm{Vol}(\mathrm{BP}(T))$ whenever $\operatorname{diam} T\le 3$. We then analyze the convexity of the connected components of $\mathrm{BP}_L^E(T)$, showing that $\mathrm{BP}_L^E(T)$ is convex whenever $\operatorname{diam} T\le 3$ but $\mathrm{BP}_L^E(P_n)$ is not convex for $n\ge 5$.

3.1. **Boundary of $\mathrm{BP}_L(T)$.** Using the parametrizations of $\mathrm{CP}_L(T)$, there is an easy analytic description of the subspace $\mathrm{BP}_L(T)$.

For $\ell\ge 2$, define the constraint function $C_\ell\colon \mathbb{R}^{\ell-1}\to\mathbb{R}$ to be

$$C_\ell(x_1,\dots,x_{\ell-1}) \coloneqq \frac{\ell-1}{2}+\sum_{1\le j\le k\le \ell-1}(-1)^{k-j+1}\cos\left(\sum_{i=j}^{k}x_i\right).$$

Lemma 3.1. *Let $\mathcal{P}\in\mathrm{CP}_L(T)$. Then $\mathcal{P}\in\mathrm{BP}_L(T)$ if and only if*

$$C_\ell(\varphi_{v_0v_1v_2},\varphi_{v_1v_2v_3},\dots,\varphi_{v_{\ell-2}v_{\ell-1}v_\ell})>0$$

holds for all paths $v_0v_1\dots v_\ell$ of length $\ell\ge 2$ in T.

Proof. For $\ell\ge 2$, define the function $F_\ell\colon\mathbb{R}^\ell\to\mathbb{R}$ to be

$$F_\ell(y_1,\dots,y_\ell)\coloneqq\frac{\ell-1}{2}+\sum_{1\le j<k\le\ell}\cos(y_k-y_j).$$

This function satisfies the relation

$$F_\ell(\theta_{v_0v_1},\theta_{v_1v_2},\dots,\theta_{v_{\ell-1}v_\ell})=C_\ell(\varphi_{v_0v_1v_2},\varphi_{v_1v_2v_3},\dots,\varphi_{v_{\ell-2}v_{\ell-1}v_\ell}).$$

To see why, recall from Remark 2.1 that

$$\varphi_{v_{i-1}v_iv_{i+1}} \equiv \theta_{v_iv_{i+1}} - \theta_{v_iv_{i-1}} \equiv \theta_{v_iv_{i+1}} - \theta_{v_{i-1}v_i} + \pi \pmod{2\pi}.$$

Thus

$$\begin{aligned}\cos(\theta_{v_{k-1}v_k} - \theta_{v_{j-1}v_j}) &= \cos\left(\sum_{i=j}^{k-1}(\theta_{v_iv_{i+1}} - \theta_{v_{i-1}v_i})\right)\\ &= \cos\left(\sum_{i=j}^{k-1}(\varphi_{v_{i-1}v_iv_{i+1}} - \pi)\right)\\ &= (-1)^{k-j}\cos\left(\sum_{i=j}^{k-1}\varphi_{v_{i-1}v_iv_{i+1}}\right).\end{aligned}$$

Summing over $1 \le j < k \le \ell$ and shifting indices proves the relation.

Thus it suffices to prove that $\mathcal{P} \in \mathrm{BP}_L(T)$ if and only if $F_\ell(\theta_{v_0v_1}, \theta_{v_1v_2}, \dots, \theta_{v_{\ell-1}v_\ell}) > 0$ holds for all paths $v_0v_1\dots v_\ell$ of length $\ell \ge 2$ in T. Observe that

$$\begin{aligned}8F_\ell(y_1,\dots,y_\ell) &= 4\ell - 4 + 8\sum_{1\le j<k\le\ell}\cos(y_j)\cos(y_k) + \sin(y_j)\sin(y_k)\\ &= \left(2\sum_{j=1}^{\ell}\cos(y_j)\right)^2 + \left(2\sum_{j=1}^{\ell}\sin(y_j)\right)^2 - 4.\end{aligned}$$

When $(y_1,\dots,y_\ell) = (\theta_{v_0v_1}, \theta_{v_1v_2}, \dots, \theta_{v_{\ell-1}v_\ell})$, this expression is equal to $(O_{v_0}O_{v_\ell})^2 - 4$. This is because $\overrightarrow{O_{v_{j-1}}O_{v_j}} = (2\cos(\theta_{v_{j-1}v_j}), 2\sin(\theta_{v_{j-1}v_j}))$, so summing up the vector for $j = 1,\dots,\ell$ gives that

$$\overrightarrow{O_{v_0}O_{v_\ell}} = \left(2\sum_{j=1}^{\ell}\cos(\theta_{v_{j-1}v_j}), 2\sum_{j=1}^{\ell}\sin(\theta_{v_{j-1}v_j})\right).$$

It follows that the distance $O_{v_0}O_{v_\ell}$ is greater than 2 if and only if $F_\ell(\theta_{v_0v_1}, \theta_{v_1v_2}, \dots, \theta_{v_{\ell-1}v_\ell}) > 0$. The lemma follows. □

The first two constraint functions are actually linear constraints.

Lemma 3.2. *Suppose that $x_1 \in [0, 2\pi)$. Then*

$$C_2(x_1) > 0 \iff \frac{\pi}{3} < x_1 < \frac{5\pi}{3}.$$

Suppose that $x_1, x_2 \in (0, 2\pi)$. Then

$$C_3(x_1, x_2) > 0 \iff \pi < x_1 + x_2 < 3\pi.$$

Proof. The linear equivalent of C_2 is clear because $C_2(x_1) = \frac{1}{2} - \cos(x_1)$. We turn our attention to C_3. Observe that

$$\begin{aligned}C_3(x_1,x_2) &= 1 - \cos(x_1) - \cos(x_2) + \cos(x_1+x_2)\\ &= 2\cos^2\left(\frac{x_1+x_2}{2}\right) - 2\cos\left(\frac{x_1+x_2}{2}\right)\cos\left(\frac{x_1-x_2}{2}\right)\\ &= 2\cos\left(\frac{x_1+x_2}{2}\right)\left(\cos\left(\frac{x_1+x_2}{2}\right) - \cos\left(\frac{x_1-x_2}{2}\right)\right)\\ &= -4\cos\left(\frac{x_1+x_2}{2}\right)\sin\left(\frac{x_1}{2}\right)\sin\left(\frac{x_2}{2}\right)\end{aligned}$$

where standard trigonometric identities are applied. By the constraints, both sine terms are positive, so we require $\cos\left(\frac{x_1+x_2}{2}\right) < 0$ with $0 < \frac{x_1+x_2}{2} < 2\pi$. This gives that $\pi < x_1 + x_2 < 3\pi$ as desired. □

Remark 3.3. It is fine to assume that x_1 and x_2 are in $(0, 2\pi)$ instead of $[0, 2\pi)$ for C_3 because we will only ever see the condition $C_3(x_1, x_2) > 0$ when we also are working with the conditions $C_2(x_1) > 0$ and $C_2(x_2) > 0$.

Remark 3.4. The fact that $C_2 > 0$ and $C_3 > 0$ are linear constraints stems from the fact that equilateral triangles and quadrilaterals have linear angle conditions. In particular, the interior angles of equilateral triangles are all $\frac{\pi}{3}$ and adjacent interior angles of equilateral quadrilaterals (also known as rhombi) sum to π.

Figure 8 displays the plots of $\mathrm{BP}_L^E(T)$ as subsets of $[0, 2\pi)^{n-1}$ for all trees T of order 4 and 5, with the irrelevant variable φ_2 factored out.

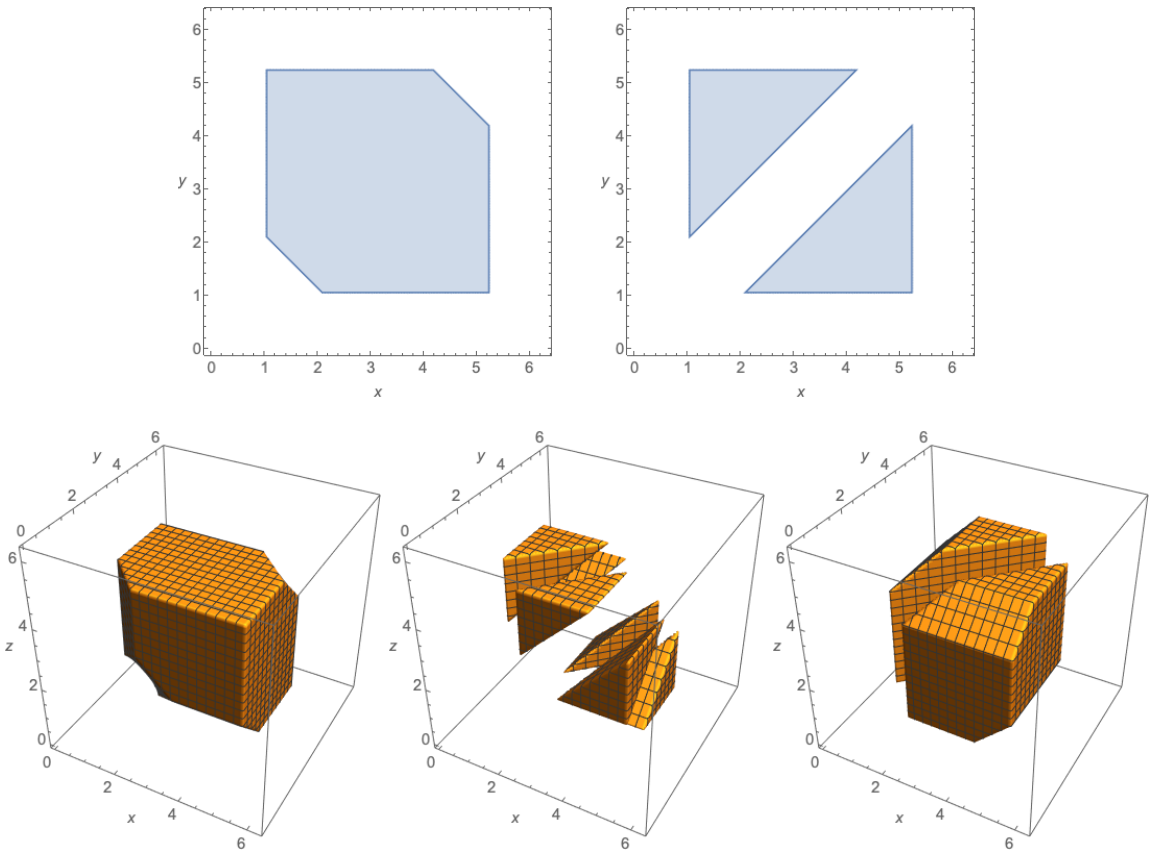

Figure 8. Plots of $\mathrm{BP}_L^E(T)$ for all trees of order 4 and 5. From left to right and first row to second row, the graphs are P_4, S_3, P_5, S_4, and $S_{2,1}$. Here, the first parameter φ_2 is omitted because there is no constraint involving it. In the plots, φ_3 is on the x-axis, φ_4 is on the y-axis, and φ_5 (if applicable) is on the z-axis.

Combining Lemmas 3.1 and 3.2 gives the following result:

Corollary 3.5. *Consider a branched polymer in* $\mathrm{BP}_L(T)$. *Then* $\frac{\pi}{3} < \varphi_{v_0v_1v_2} < \frac{5\pi}{3}$ *for any path* $v_0v_1v_2$ *of length* 2 *in* T *and* $\pi < \varphi_{v_0v_1v_2} + \varphi_{v_1v_2v_3} < 3\pi$ *for any path* $v_0v_1v_2v_3$ *of length* 3 *in* T.

It follows from these linear constraints that for any tree with diameter at most 3, the set $\mathrm{BP}_L^E(T)$ is the union of polytopes. Consequently, the volume $V_L(T)$ can be computed with a straightforward integral. We defer the calculation to Appendix A and present the values in Table 1.

n	T	$V_L(T)$	$\mathrm{Aut}(T)$	$\mathrm{Vol}(\mathrm{BP}(T))$
1	P_1	1	Triv	$(2\pi)^0$
2	$P_2 = S_1$	2π	Dih_1	$(2\pi)^1$
3	$P_3 = S_2$	$\frac{8\pi^2}{3}$	Dih_1	$2(2\pi)^2$
4	S_3	$2\pi^3$	Sym_3	$2(2\pi)^2$
	$P_4 = S_{1,1}$	$\frac{10\pi^3}{3}$	Dih_1	$4(2\pi)^3$
5	S_4	$\frac{16\pi^4}{27}$	Sym_4	$\frac{5}{27}(2\pi)^4$
	$S_{2,1}$	$\frac{184\pi^4}{81}$	Sym_2	$\frac{230}{27}(2\pi)^4$
6	S_5	$\frac{2\pi^5}{81}$	Sym_5	$\frac{1}{216}(2\pi)^5$
	$S_{3,1}$	$\frac{47\pi^5}{81}$	Sym_3	$\frac{235}{108}(2\pi)^5$
	$S_{2,2}$	$\frac{322\pi^5}{243}$	$\mathrm{Dih}_1 \times S_2^2$	$\frac{805}{216}(2\pi)^5$
7	$S_{4,1}$	$\frac{8\pi^6}{405}$	Sym_4	$\frac{7}{108}(2\pi)^6$
	$S_{3,2}$	$\frac{104\pi^6}{405}$	$\mathrm{Sym}_3 \times \mathrm{Sym}_2$	$\frac{91}{54}(2\pi)^6$
8	$S_{4,2}$	$\frac{4\pi^7}{729}$	$\mathrm{Sym}_4 \times \mathrm{Sym}_2$	$\frac{35}{972}(2\pi)^7$
	$S_{3,3}$	$\frac{98\pi^7}{3645}$	$\mathrm{Dih}_1 \times \mathrm{Sym}_3^2$	$\frac{343}{2916}(2\pi)^7$
9	$S_{4,3}$	$\frac{8\pi^8}{76545}$	$\mathrm{Sym}_4 \times \mathrm{Sym}_3$	$\frac{1}{972}(2\pi)^8$

Table 1. The volumes for each tree with diameter at most 3 and positive volume.

Since the only trees of order 5, up to isomorphism, are S_4, $S_{2,1}$, and P_5, we can use Table 1 to compute that

$$\mathrm{Vol}(\mathrm{BP}(P_5)) = \left(24 - \frac{5}{27} - \frac{230}{27}\right)(2\pi)^4 = \frac{413}{27}(2\pi)^4$$

and thus $V_L(P_5) = \frac{1652\pi^4}{405}$. We believe that this is the only tree with diameter at least 4 whose volume is known.

3.2. **Convexity of connected components.** One interesting inquiry about the shape of $\mathrm{BP}_L^E(T)$ is on the convexity of its connected components. If the connected components are convex, then optimization problems on the branched polymers can be resolved using known optimization algorithms on convex sets.

If a connected component is the intersection of half-spaces, then it is a convex polytope. By Corollary 3.5 of Lemma 3.2, this is true of every connected component of $\mathrm{BP}_L^E(T)$ whenever $\operatorname{diam} T \leq 3$, so the connected components are convex whenever $\operatorname{diam} T \leq 3$. Unfortunately, convexity breaks apart whenever $\operatorname{diam} T \geq 4$.

Lemma 3.6. *Under the argument parametrization, the (connected) set* $\mathrm{BP}_L^E(P_n) \subset [0, 2\pi)^{n-1}$ *is not convex for* $n \geq 5$.

Proof. We will essentially exhibit two branched polymers in $\mathrm{BP}_L(P_n)$ such that the midpoint of their representatives in $[0, 2\pi)^{n-1}$ is not in $\mathrm{BP}_L^E(P_n)$. Consider the crossing polymers with previous edge parametrizations $(\pi, \frac{5\pi}{3}, \frac{4\pi}{3}, \frac{4\pi}{3}, \frac{2\pi}{3}, \pi, \pi, \ldots, \pi)$ and $(\pi, \frac{7\pi}{5}, \frac{7\pi}{5}, \frac{7\pi}{5}, \frac{4\pi}{5}, \pi, \pi, \ldots, \pi)$. It is straightforward to verify that both are indeed branched polymers whose representatives in $[0, 2\pi)^{n-1}$ are in $\overline{\mathrm{BP}_L^E(P_n)}$, the closure of $\mathrm{BP}_L^E(P_n)$ (Figure 9).

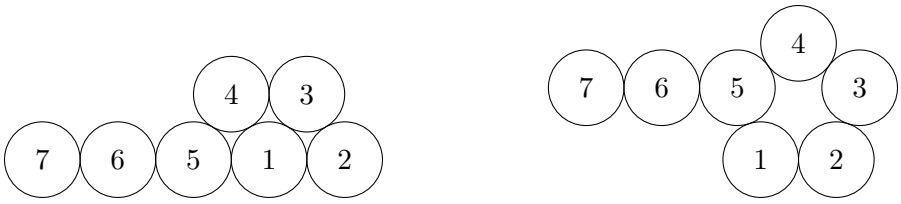

Figure 9. Two branched polymers in $\overline{\mathrm{BP}_L^E(P_7)}$.

However, the "midpoint" of these two branched polymers—the labelled crossing polymer with previous edge parametrization $(\pi, \frac{23\pi}{15}, \frac{41\pi}{30}, \frac{41\pi}{30}, \frac{11\pi}{15}, \pi, \pi, \ldots, \pi)$—does not have representative in $\overline{\mathrm{BP}_L^E(P_n)}$ (Figure 10). Indeed, it can be computed that $C_4(\varphi_3, \varphi_4, \varphi_5) \approx -0.08037$, which violates Lemma 3.1.

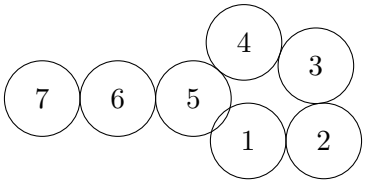

Figure 10. The midpoint is not in $\overline{\mathrm{BP}_L^E(P_7)}$.

Since the closure of a convex set is convex, the set $\mathrm{BP}_L^E(P_n)$ cannot be convex. □

Remark 3.7. This counterexample can be adjusted to provide a direct proof that $\mathrm{BP}_L^E(P_n)$ is not convex without having to resort to the closure. Indeed, subtracting a small positive constant ϵ from φ_3 provides two branched polymers whose midpoint is not a branched polymer.

See Figure 11 for a zoomed in view of $\mathrm{BP}_L^E(T)$ which displays the non-convexity.

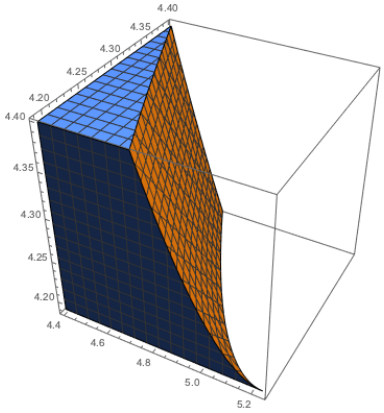

Figure 11. Plot of $\mathrm{BP}_L^E(P_5)$, zoomed in to the region $[\frac{7\pi}{5}, \frac{5\pi}{3}] \times [\frac{4\pi}{3}, \frac{7\pi}{5}] \times [\frac{4\pi}{3}, \frac{7\pi}{5}]$.

Lemma 3.6 can be adapted to show that connected components of $\mathrm{BP}_L^E(T)$ are not convex for some trees T besides path graphs. For example, the connected component corresponding to the polymer on the left in Figure 5 is not convex by this construction.

However, it is not true in general that $\operatorname{diam} T \geq 4$ implies that all connected components of $\mathrm{BP}_L^E(T)$ are not convex. Indeed, the connected component corresponding to the polymer on the right in Figure 5 is the intersection of half-spaces and is thus convex. To see why, observe that the

path of length 4 cannot ever be realized in a branched polymer in this connected component. As such, the condition C_4 never kicks in, causing the connected component to be the intersection of half-spaces.

4. Asymptotics of $V_L(T)$

In this section, we give two inequalities implying a submultiplicative-type (with respect to tree concatenation) behavior of $V_L(T)$. These inequalities connect the study of branched polymers with tangency graph P_n to that of self-avoiding walks on a lattice, allowing us to analyze the asymptotics of $V_L(T)$.

4.1. **Submultiplicative-type inequalities.** Let $G - e$ denote deletion of edge e and G/e denote contraction of vertex pair e (in contraction, e is not necessarily an edge).

Lemma 4.1. *Let T be a tree and $uv \in E(T)$. Let T_1, T_2 be trees such that $T - uv = T_1 \sqcup T_2$. Then*

$$V_L(T) \leq 2\pi V_L(T_1)V_L(T_2).$$

Proof. We provide a volume-preserving injection from $\mathrm{BP}_L(T)$ to $\mathrm{BP}_L(T_1) \times (-\pi, \pi] \times \mathrm{BP}_L(T_2)$. Take an arbitrary branched polymer $\mathcal{P}$ in $\mathrm{BP}_L(T)$. Let $\mathcal{P}_1$ denote the set of disks in $\mathcal{P}$ corresponding to T_1 and $\mathcal{P}_2$ denote the set of disks in $\mathcal{P}$ corresponding to T_2. Let C_1, C_2 be the centers of the disks corresponding to the endpoints of the edge that was removed, with $C_1 \in \mathcal{P}_1$ and $C_2 \in \mathcal{P}_2$. Then our injection is $\mathcal{P} \mapsto (\mathcal{P}_1, \operatorname{Arg} \overrightarrow{C_1C_2}, \mathcal{P}_2)$ where Arg represents principal argument (Figure 12). □

Remark 4.2. We can actually replace the constant 2π with $\frac{4\pi}{3}$ as long as $|V(T)| > 2$ since $\frac{2\pi}{3}$ of the full range of angles for $\operatorname{Arg} \overrightarrow{C_1C_2}$ is invalid.

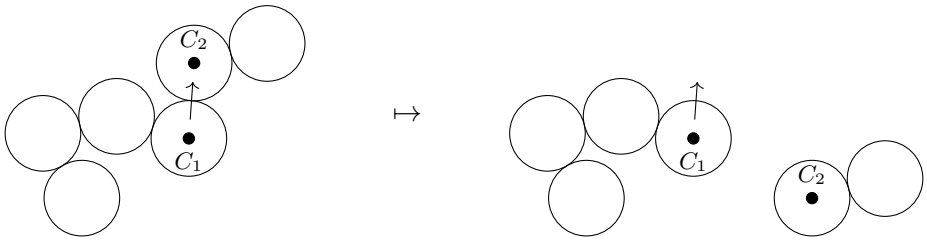

Figure 12. The injection exhibited in the proof of Lemma 4.1, demonstrated on $T = P_6$. The arrow pointing away from C_1 represents the angle of the vector $\overrightarrow{C_1C_2}$.

A similar inequality stems from edge contraction.

Lemma 4.3. *Let T be a tree. Let T_1, T_2 be trees for which there exist $u \in V(T_1)$ and $v \in V(T_2)$ such that $T = (T_1 \sqcup T_2)/uv$. Then*

$$V_L(T) \leq V_L(T_1)V_L(T_2).$$

This can be proven using a similar injection as in the proof of Lemma 4.1.

4.2. **Connective constant.** Using the submultiplicative-type inequality on $V_L(T)$, we are able to deduce the existence of a connective constant for branched polymers, akin to that of self-avoiding walks on a lattice as done by Hammersley and Morton [6]. To do this, we will use a lemma of Fekete [3].

Lemma 4.4. *Let $\{a_n\}_{n\geq 1}$ be a subadditive sequence of real numbers, i.e. $a_{m+n} \leq a_m + a_n$ for all $m, n \in \mathbb{N}$. Then*

$$\lim_{n\to\infty} \frac{a_n}{n} = \inf_{n\geq 1} \frac{a_n}{n}.$$

Given Fekete's lemma, we can show the existence of a connective constant.

Theorem 4.5. *There exists a constant $\mu \in [\frac{2\pi}{3}, \frac{4\pi}{3}]$ for which*

$$\lim_{n\to\infty} \sqrt[n]{V_L(P_n)} = \mu.$$

Proof. We can take $T = P_{m+n}$, $T_1 = P_m$, and $T_2 = P_n$ in Lemma 4.1 to get that

$$2\pi V_L(P_{m+n}) \leq 2\pi V_L(P_m) \cdot 2\pi V_L(P_n).$$

Taking the logarithm gives that $a_n = \log(2\pi V_L(P_n))$ is subadditive. Applying Lemma 4.4, we deduce that

$$\lim_{n\to\infty} \frac{\log(2\pi V_L(P_n))}{n} \text{ exists and is in } [-\infty, \infty).$$

Exponentiating, we deduce that $\lim_{n\to\infty} \sqrt[n]{V_L(P_n)} = \mu$ for some $\mu \geq 0$.

Now, we show that

$$2\pi \cdot \left(\frac{2\pi}{3}\right)^{n-2} \leq V_L(P_n) \leq 2\pi \cdot \left(\frac{4\pi}{3}\right)^{n-2}$$

for $n \geq 2$, which would imply the bounds on μ.

We first show the upper bound. Observe that $V_L(P_{n+1}) \leq \frac{4\pi}{3} V_L(P_n)$ for $n \geq 2$. Indeed, φ_{n+1} must be between $\frac{\pi}{3}$ and $\frac{5\pi}{3}$. Combined with the fact that $V_L(P_2) = 2\pi$, the upper bound follows.

Now, we show the lower bound. Situate a coordinate axes such that O_1 is at the origin and O_2 is on the positive x-axis. The key claim is that by taking $\theta_k \in (0, \frac{2\pi}{3})$ for $k = 3, \ldots, n$, we generate a valid polymer. By induction, it suffices to show that $O_k O_n > 2$ for each $k \leq n-2$.

Observe that $|\theta_n - \theta_{n-1}| < \frac{2\pi}{3}$ by construction, so $\varphi_n = \pi + \theta_n - \theta_{n-1}$ lies strictly between $\frac{\pi}{3}$ and $\frac{5\pi}{3}$. By Lemmas 3.1 and 3.2, this implies that $O_{n-2}O_n > 2$ so it remains to show the inequality for $k \leq n-3$. We casework on the number of $m > k$ such that $\theta_m > \frac{\pi}{6}$.

- There are no such indices $m > k$. Then both coordinates of $\overrightarrow{O_{i-1}O_i}$ are non-negative for $i > k$. It follows that both coordinates of $\overrightarrow{O_kO_n}$ are at least the corresponding (non-negative) coordinates of $\overrightarrow{O_{n-1}O_n}$, so $O_kO_n > O_{n-1}O_n = 2$.
- There is exactly one such index $m > k$. Then the x-coordinate of $\overrightarrow{O_{i-1}O_i}$ is at least $\sqrt{3}$ for $i > k$ besides m, while the x-coordinate of $\overrightarrow{O_{m-1}O_m}$ is greater than -1. Thus the x-coordinate of $\overrightarrow{O_kO_n}$ is greater than

  $$(n-k-1) \cdot \sqrt{3} + 1 \cdot (-1) \geq 2\sqrt{3} - 1 > 2,$$

  so $O_kO_n > 2$.
- There are at least two such indices $m > k$. Observe that the y-coordinate of $\overrightarrow{O_{i-1}O_i}$ is always non-negative for $i > k$. Furthermore, if $\theta_m > \frac{\pi}{6}$ then the y-coordinate of $\overrightarrow{O_{m-1}O_m}$ is greater than 1. It follows that the y-coordinate of $\overrightarrow{O_kO_n}$ is greater than 2, so $O_kO_n > 2$.

Thus a valid polymer is generated this way, implying the lower bound. □

It is conjectured (e.g. Jensen [7]) that if c_n is the number of self-avoiding random walks of length n on a lattice Λ, then

$$c_n \sim A\mu^n n^{\gamma-1}$$

where A and μ depend on Λ but γ is a universal constant. Because of the resemblance between branched polymers with tangency graph P_n and self-avoiding walks, we conjecture that a similar asymptotic holds for $V_L(P_n)$. Based on experimental data, the value of μ appears to be around 0.58.

5. Zero-volume trees

We say that a tree T is a **zero-volume tree** if $V_L(T) = 0$. Note that T being a zero-volume tree implies that there is no branched polymer with tangency graph T. This is because $\mathrm{BP}_L^E(T)$ is an open subset of $[0, 2\pi)^{n-1}$, and non-empty open sets have positive volume. Contrast this with general graphs G; for example, $V_L(K_3) = 0$ where K_3 is the triangle graph, but there exist branched polymers with tangency graph K_3.

If T is a zero-volume tree, then any tree T' that contains T as a subgraph is also a zero-volume tree. We say that a tree T is a **primitive zero-volume tree** if no proper subgraph of T is zero-volume. Then the set of zero-volume trees is precisely the set of trees which have some primitive zero-volume tree as a subgraph. Thus to analyze zero-volume trees, it suffices to identify the primitive zero-volume trees.

We show that the values that $\Delta(T)$ takes on over all primitive zero-volume trees T are $\{3, 4, 5, 6\}$, where $\Delta(T)$ is the maximum degree of T. To do this, we provide several zero-volume trees using two main methods. One way is to find a circle of small radius which must enclose any branched polymer with given tangency graph and create a contradiction using this. Another method, stronger than the first, is to use a constructive geometric argument by adding up angles and arriving at a contradiction.

5.1. **Disk packing arguments.** Zero-volume trees can come from the branched polymer being "too crowded," i.e. violating a disc packing inequality. For a positive integer m, let $r(m)$ denote the radius of the smallest circle in which m unit disks can be packed.

For example, Graham [4] proved that $r(7) = 3$, with optimal configuration as shown in Figure 13.

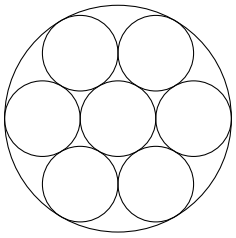

Figure 13. The optimal packing of 7 unit disks in a circle.

From this, it follows that no branched polymer can have tangency graph S_6. Indeed, the triangle inequality implies that any branched polymer in $\mathrm{BP}(S_6)$ must lie within a circle of radius 3. But the optimal packing of 7 disks forces such a branched polymer to instead have a tangency graph with cycles. Thus S_6 is zero-volume. This forces $\Delta(T) \leq 5$ for any tree T with positive volume.

Additionally, since S_a for $a < 6$ has positive volume, the following theorem is true:

Theorem 5.1. *The tree S_6 is a primitive zero-volume tree.*

This argument to identify zero-volume trees can be generalized by the following lemma:

Lemma 5.2. *If $r(n) > \operatorname{diam} T + 1$ where n is the order of T, then T is zero-volume.*

Proof. Let $d = \operatorname{diam} T$. The key claim is that a branched polymer with tangency graph T fits inside a circle of radius $d + 1$. Take a path $v_0 v_1 \dots v_d$ of length d in T. We will prove that if O is the midpoint of broken line $O_{v_0} O_{v_1} \dots O_{v_d}$, then the center of every disk lies in a closed circle of radius d centered at O. Casework on whether d is even or odd.

- Suppose $d = 2k$ is even, then O is O_{v_k}. By construction, the eccentricity of v_k is k. Since each edge in T corresponds to a segment between disk centers of length 2, there is a broken

line from O to every disk center with length at most $2k = d$ and thus a straight line with length at most d.

- Suppose $d = 2k + 1$ is odd, then O is the midpoint of $O_{v_k}O_{v_{k+1}}$. By construction, the eccentricity of v_k is $k+1$. Furthermore, if the distance from v_k to another vertex is exactly $k + 1$, then the path must use edge v_kv_{k+1}—otherwise the distance from v_d to this other vertex is $2(k+1) = d+1$. It follows that there is a broken line from O to every disk center with length at most $2k + 1 = d$ and thus a straight line with length at most d.

Thus the distance from O to every disk center is at most d, so applying the triangle inequality again provides that the distance from O to every point in a disk is at most $d + 1$. The contrapositive of the lemma statement follows directly. □

An immediate bound on $r(n)$ is that $r^2 \geq n$ (by comparing areas). A slightly less obvious bound comes from the fact that the densest packing of circles in the plane is the hexagonal packing. As shown by Tóth [2], we actually have $r^2 \geq \frac{\sqrt{12}}{\pi}n$. This inequality was strengthened by Groemer [5] to

$$n\sqrt{12} \leq \pi r^2 - (2 - \sqrt{3})\pi r + \sqrt{12} - \pi \cdot (\sqrt{3} - 1).$$

Using these bounds, we can identify some zero-volume trees. A d-quasi-regular tree is a tree for which every vertex has degree in $\{1, d\}$. The **complete d-quasi-regular tree of height** h is the d-quasi-regular tree generated by a level structure with levels 0 through h such that level k for $k \geq 1$ has the maximal $d \cdot (d-1)^{k-1}$ vertices (Figure 14).

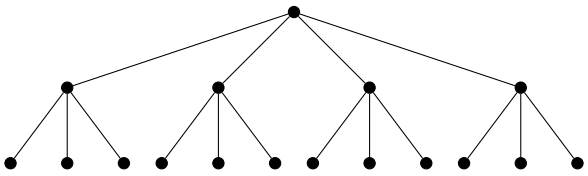

Figure 14. The complete 4-quasi-regular tree of height 2.

Observe that the complete d-quasi-regular tree of height h has $1 + d \cdot \frac{(d-1)^h-1}{d-2}$ vertices and diameter $2h$. By applying Lemma 5.2 and the bound $r(n) \geq \sqrt{n}$, we have the following results.

Corollary 5.3. *The complete* 3*-quasi-regular tree of height* 6 *is zero-volume.*

Corollary 5.4. *The complete* 4*-quasi-regular tree of height* 3 *is zero-volume.*

These results demonstrate the existence of zero-volume trees with $\Delta(T) = 3$ and $\Delta(T) = 4$, respectively.

5.2. **Constructive geometric arguments.** Some geometric arguments utilizing angle conditions can also be employed to find zero-volume trees. For example, Theorem 5.1 can alternatively be proven by noting that the six angles between consecutive leaves must each be greater than $\frac{\pi}{3}$ while their sum is 2π, leading to a contradiction.

We can prove a similar result on one of the trees with diameter 3.

Theorem 5.5. *The tree $S_{4,4}$ is a primitive zero-volume tree.*

Proof. First, observe that all possible connected components of $\mathrm{BP}_L(S_{4,4})$ must be congruent. This is true because there is a correspondence between elements of different connected components that preserves the geometric shape of the branched polymer, thus preserving the shape of the connected component.

Suppose that there exists a branched polymer with $S_{4,4}$ as its tangency graph. Consider the labelling of $S_{4,4}$ in Figure 15 and look at the connected component with edges ordered in the same order as in the diagram.

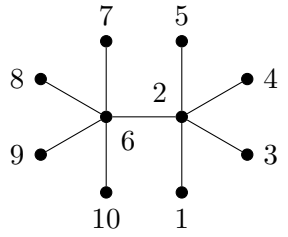

Figure 15. Labelling and ordering of $S_{4,4}$.

Recall Corollary 3.5 of Lemma 3.2, which states that $\frac{\pi}{3} < \varphi_{v_0v_1v_2} < \frac{5\pi}{3}$ for any path $v_0v_1v_2$ of length 2 and $\pi < \varphi_{v_0v_1v_2} + \varphi_{v_1v_2v_3} < 3\pi$ for any path $v_0v_1v_2v_3$ of length 3. Using the conversion between φ_{uvw} and φ_v, we require

$$\begin{aligned} \varphi_3, \varphi_4 - \varphi_3, \varphi_5 - \varphi_4 &> \frac{\pi}{3} \\ (\varphi_6 - \varphi_5) + \varphi_7 &> \pi \\ \varphi_8 - \varphi_7, \varphi_9 - \varphi_8, \varphi_{10} - \varphi_9 &> \frac{\pi}{3} \\ \varphi_6 + \varphi_{10} &< 3\pi. \end{aligned}$$

However, adding up all seven inequalities in the first three lines contradicts the fourth line, so $S_{4,4}$ is zero-volume. From Table 1, it follows that $S_{4,4}$ is a primitive zero-volume tree. □

Now, we exhibit a refinement of Corollary 5.4 which provides a primitive zero-volume tree with $\Delta(T) = 4$.

Theorem 5.6. *The complete* 4*-quasi-regular tree of height* 2 *is a primitive zero-volume tree.*

To prove this, we will first need two geometric lemmas whose proofs we defer to Appendix B.

Lemma 5.7. *Consider a branched polymer with tangency graph* S_4 *such that the center is labelled as* 2 *and the leaves are labelled as* $1, 3, 4, 5$ *in counterclockwise order. Then* $\angle O_3O_1O_5 > \frac{\pi}{3}$.

Lemma 5.8. *Consider a branched polymer with tangency graph* P_5 *labelled in order. Suppose that* $\varphi_2, \varphi_3, \varphi_4 < \pi$. *Then* $\angle O_1O_3O_5 > \frac{\pi}{6}$.

Given these two lemmas, we can now prove Theorem 5.6.

Proof of Theorem 5.6. First, observe that all possible connected components of the complete 4-quasi-regular tree of height 2 must be congruent. This is true for the same reasons as mentioned in the proof of Theorem 5.5 (a correspondence exists between elements of different connected components that preserves the shape of the connected component).

Suppose that there exists a branched polymer with this tree as its tangency graph. Consider the labelling of the graph in Figure 16 and look at the connected component with edges ordered in the same order as in the diagram.

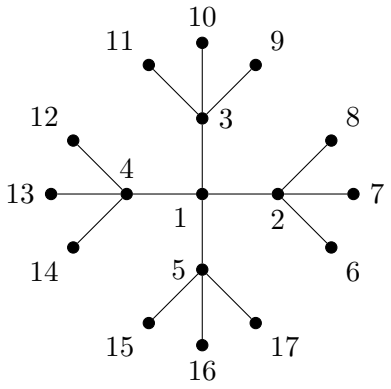

Figure 16. Labelling and ordering of the complete 4-quasi-regular tree of height 2.

Observe that the branched polymers induced by $\{1, 2, 6, 7, 8\}$, $\{1, 3, 9, 10, 11\}$, etc. are all S_4. Thus by Lemma 5.7, we have

$$\angle O_6O_1O_8, \angle O_9O_1O_{11}, \angle O_{12}O_1O_{14}, \angle O_{15}O_1O_{17} > \frac{\pi}{3}$$

when these angles are measured counterclockwise. Additionally observe that the branched polymers induced by $\{8, 2, 1, 3, 9\}$, $\{11, 3, 1, 4, 12\}$, etc. satisfy the conditions in Lemma 5.8. It follows by this lemma that

$$\angle O_8O_1O_9, \angle O_{11}O_1O_{12}, \angle O_{14}O_1O_{15}, \angle O_{17}O_1O_6 > \frac{\pi}{6}$$

when these angles are measured counterclockwise. Adding these eight inequalities results in 2π on both sides of the strict inequality, which is a contradiction. Thus the complete 4-quasi-regular tree of height 2 is zero-volume.

To show that the tree is a primitive zero-volume tree, it suffices to show that the tree formed by removing one leaf has positive probability. Figure 17 demonstrates why this is true.

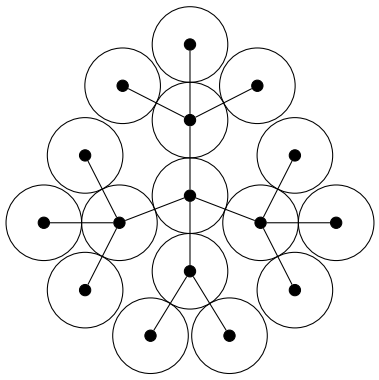

Figure 17. The 4-quasi-regular tree of height 2, upon removing a leaf, no longer remains zero-volume.

Consequently, the 4-quasi-regular tree of height 2 is a primitive zero-volume tree. □

By combining the results in this section, we have the following theorem:

Theorem 5.9. *Let m be a positive integer. There exists a primitive zero-volume tree with $\Delta(T) = m$ if and only if $m \in \{3, 4, 5, 6\}$.*

Proof. The constructions for $m \in \{4, 5, 6\}$ are provided by Theorems 5.6, 5.5, and 5.1, respectively. For $m = 3$, observe that there exists a zero-volume tree with $\Delta(T) = 3$ by Corollary 5.3. Some subgraph of this tree must be a primitive zero-volume tree. But this primitive zero-volume tree cannot have $\Delta(T) \leq 2$, so it must have $\Delta(T) = 3$.

Observe that $m \leq 2$ is impossible as the only trees with $\Delta(T) \leq 2$ are the path graphs, which have positive volume. In addition, any tree with $\Delta(T) \geq 7$ has S_6 as a proper subgraph and hence cannot be a primitive zero-volume tree. The theorem follows. □

Remark 5.10. In these constructive arguments using angles, the key is understanding the boundary of $\mathrm{BP}_L(T)$. Indeed, to prove each of Theorems 5.1, 5.5, and 5.6, the argument essentially identifies a polymer that "should be" a limit point of $\mathrm{BP}_L(T)$ (Figure 18).

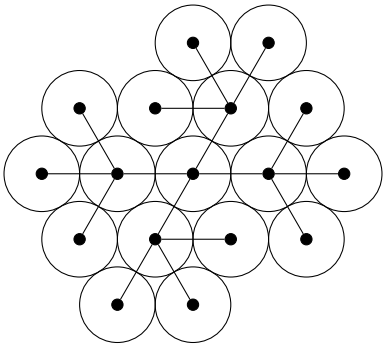

Figure 18. This branched polymer "should be" a limit point of $\mathrm{BP}_L(T)$ where T is the complete 4-quasi-regular tree of height 2. However, there is no room to "wiggle around" the tangent disks, suggesting that $\mathrm{BP}_L(T)$ is actually empty. This intuitive argument can be formalized by algebraically describing the lack of space, which is what occurs in the proof of Theorem 5.6.

Remark 5.10 suggests a method for generating zero-volume trees: Let H be a finite subtree of the infinite triangular lattice graph, and add all neighbors of H not already in H to this tree as leaves. Then the resulting tree may be zero-volume.

Indeed, this method works when we choose a single vertex as H (resulting in S_6), or P_2 (resulting in $S_{4,4}$), or the X-shaped formation of S_4 (resulting in the complete 4-quasi-regular tree of height 2).

However, this method does not work in general. Choosing the V-shaped formation of P_3 and adding the neighbors as in Figure 19 does not generate a zero-volume tree.

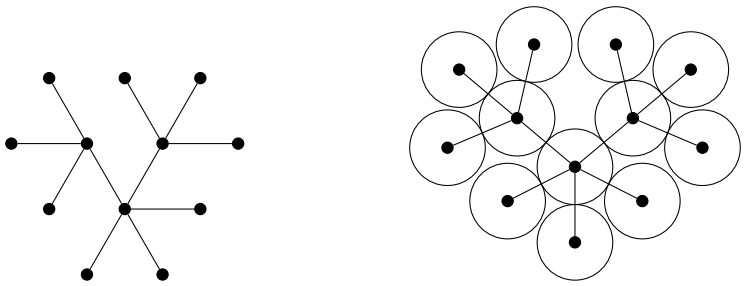

Figure 19. The method to generate zero-volume trees fails in this case.

Appendix A. Trees with diameter at most 3

Using the relations in Corollary 3.5 of Lemma 3.2, it is straightforward to compute the volume $V_L(T)$ for every tree T with $\operatorname{diam} T \leq 3$. We will use the previous edge parametrization, defining some auxiliary variables which will make computation easier.

The only tree with diameter 1 is the trivial graph, which has volume 1. The trees with diameter 2 are S_a for $a \geq 2$. In order for S_a to have positive volume, we require $a \leq 5$ by Theorem 5.1.

We now compute $V_L(S_a)$. Note that all $(a-1)!$ connected components are identical. Consider the labelling and connected component such that the center of the star is labelled as 2 and the leaves labelled as $1, 3, 4, \ldots, a+1$ in counterclockwise order. Then the constraints are that

$$\frac{\pi}{3} < \varphi_3, \varphi_4 - \varphi_3, \ldots, \varphi_{a+1} - \varphi_a, 2\pi - \varphi_{a+1} < \frac{5\pi}{3}.$$

Define $\phi_3 = \varphi_3$ and $\phi_k = \varphi_k - \varphi_{k-1}$ for $k = 4, \ldots, a+1$. Then we require

$$\phi_3, \ldots, \phi_{a+1} > \frac{\pi}{3} \quad \text{and} \quad \phi_3 + \cdots + \phi_{a+1} < \frac{5\pi}{3}.$$

The $(a-1)$-dimensional space satisfying these conditions is the interior of a standard $(a-1)$-simplex with side length $2\pi - \frac{a\pi}{3}$. Since a standard d-simplex with side length s has volume $\frac{s^d}{d!}$, we deduce that

$$\frac{V_L(S_a)}{(a-1)!} = 2\pi \cdot \frac{(2\pi - \frac{a\pi}{3})^{a-1}}{(a-1)!}$$

where the factor of 2π comes from φ_2, so

$$V_L(S_a) = 2\pi \cdot (2\pi - \frac{a\pi}{3})^{a-1}.$$

Now, we turn our attention to the trees with diameter 3, which are $S_{a,b}$ for $a, b \geq 1$. For $S_{a,b}$ to have positive volume, we require $a, b \leq 4$ by Theorem 5.1. Furthermore, $a = b = 4$ is impossible by Theorem 5.5. Henceforth we assume that $4 \geq a \geq b \geq 1$ and $b < 4$.

We now compute $V_L(S_{a,b})$. Note that all $a!b!$ connected components are identical. Consider the labelling and connected component such that the center of the subgraph S_a is labelled as $a+2$ and the center of the subgraph S_b is labelled as 2, with the neighbors of vertex $a+2$ labelled as $2, a+3, a+4, \ldots, a+b+2$ in counterclockwise order and the neighbors of vertex 2 labelled as $1, 3, 4, \ldots, a+1$ in counterclockwise order (Figure 20).

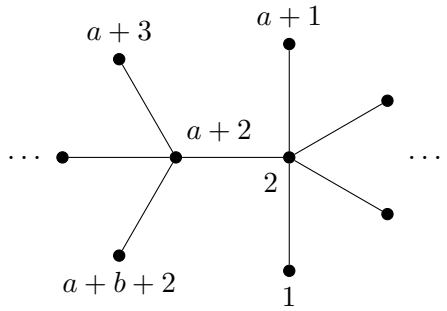

Figure 20. Labelling and ordering of $S_{a,b}$.

Then the constraints are that

$$\begin{aligned}
&\frac{\pi}{3} < \varphi_3, \varphi_4 - \varphi_3, \dots, \varphi_{a+1} - \varphi_a < \frac{5\pi}{3} \\
&\pi < (\varphi_{a+2} - \varphi_{a+1}) + \varphi_{a+3} < 3\pi \\
&\frac{\pi}{3} < \varphi_{a+4} - \varphi_{a+3}, \dots, \varphi_{a+b+2} - \varphi_{a+b+1} < \frac{5\pi}{3} \\
&\pi < \varphi_{a+2} + \varphi_{a+b+2} < 3\pi.
\end{aligned}$$

Define $\alpha = \varphi_{a+b+2} - \varphi_{a+3}$, $\beta = \varphi_{a+1}$, $\theta = \varphi_{a+3}$, and $\omega = \varphi_{a+2} - \varphi_{a+1}$. Additionally define $\phi_3 = \varphi_3$ and $\phi_k = \varphi_k - \varphi_{k-1}$ for $k = 4, \dots, a, a+4, \dots, a+b+1$. Suppose that $a, b > 1$. Then the constraints become the following conditions:

(1) $(a-1)\frac{\pi}{3} < \alpha < \frac{4\pi}{3}$
(2) $(b-1)\frac{\pi}{3} < \beta < \frac{4\pi}{3}$
(3) $\frac{\pi}{3} < \theta < \frac{5\pi}{3} - \alpha$
(4) $\frac{\pi}{3} < \omega < \frac{5\pi}{3} - \beta$
(5) $\pi < \theta + \omega < 3\pi - \alpha - \beta$
(5') consequently, $\alpha + \beta < 2\pi$
(6) $\phi_3, \dots, \phi_a > \frac{\pi}{3}$
(7) $\phi_3 + \cdots + \phi_a < \alpha - \frac{\pi}{3}$
(8) $\phi_{a+4}, \dots, \phi_{a+b+1} > \frac{\pi}{3}$
(9) $\phi_{a+4} + \cdots + \phi_{a+b+1} < \beta - \frac{\pi}{3}$

Let $\mathcal{R}$ be the 2-dimensional region defined by conditions 1, 2, and 5'. For fixed α, β, let $\mathcal{R}_1$ be the region defined by conditions 3, 4, and 5; let $\mathcal{R}_2$ be the region defined by conditions 6 and 7; let $\mathcal{R}_3$ be the region defined by conditions 8 and 9. Then the volume of the connected component is

$$2\pi \cdot \int_{\mathcal{R} \times \mathcal{R}_1 \times \mathcal{R}_2 \times \mathcal{R}_3} \mathrm{d}V = 2\pi \cdot \int_{\mathcal{R}} \mathrm{Vol}(\mathcal{R}_1)\,\mathrm{Vol}(\mathcal{R}_2)\,\mathrm{Vol}(\mathcal{R}_3)\,\mathrm{d}\alpha\,\mathrm{d}\beta.$$

We can directly compute the three volumes in the integrand. We have that

$$\mathrm{Vol}(\mathcal{R}_1) = \frac{(\frac{7\pi}{3} - \alpha - \beta)^2}{2} - \frac{(\frac{\pi}{3})^2}{2} - \frac{(\pi - \alpha)^2}{2} \cdot \mathrm{sgn}(\pi - \alpha) - \frac{(\pi - \beta)^2}{2} \cdot \mathrm{sgn}(\pi - \beta)$$

where $\mathrm{sgn}(x)$ is the signum function. Indeed, this formula can be verified by looking at each of the cases depending on if α, β are less than or greater than π. Only two cases need to be checked: $\alpha < \pi, \beta < \pi$ and $\alpha < \pi, \beta > \pi$, as $\alpha > \pi, \beta < \pi$ is symmetrical to the second case and $\alpha > \pi, \beta > \pi$ is impossible by condition 5'.

Now, note that $\mathcal{R}_2$ and $\mathcal{R}_3$ are standard simplexes, so

$$\mathrm{Vol}(\mathcal{R}_2) = \frac{(\alpha - \frac{(a-1)\pi}{3})^{a-2}}{(a-2)!} \quad \text{and} \quad \mathrm{Vol}(\mathcal{R}_3) = \frac{(\beta - \frac{(b-1)\pi}{3})^{b-2}}{(b-2)!}.$$

Combining these volumes, we can integrate and thus compute $V_L(S_{a,b})$ for $a, b > 1$.

In the case that $a > 1$ and $b = 1$, we can instead note that β is forced to be 0 and $\mathrm{Vol}(\mathcal{R}_3) = 1$, with the rest of the formula working the same way. When $a = b = 1$, we have that $\alpha = \beta = 0$ and $\mathrm{Vol}(\mathcal{R}_2) = \mathrm{Vol}(\mathcal{R}_3) = 1$, so the integral instead just requires plugging in $(\alpha, \beta) = (0, 0)$ to the formula for $\mathrm{Vol}(\mathcal{R}_1)$.

Thus we can compute $V_L(T)$ whenever $\operatorname{diam} T \leq 3$. The information is collected in Table 1.

Appendix B. Proofs of Lemmas 5.7 and 5.8

In this appendix, we provide proofs of Lemmas 5.7 and 5.8. We freely apply Corollary 3.5 of Lemma 3.2 to prove these lemmas.

Proof of Lemma 5.7. Observe that O_2 is the circumcenter of $\triangle O_1O_3O_5$. By a well-known fact about circumcenters, $\angle O_3O_2O_5 = 2\angle O_3O_1O_5$. But

$$\angle O_3O_2O_5 = \angle O_3O_2O_4 + \angle O_4O_2O_5 > \frac{\pi}{3} + \frac{\pi}{3},$$

so $\angle O_3O_1O_5 > \frac{\pi}{5}$ as desired. □

Proof of Lemma 5.8. For convenience, let $\alpha = \varphi_2$, $\beta = \varphi_4$, $\theta = \varphi_3$, and $\gamma = \angle O_1O_3O_5$ (Figure 21). Without loss of generality, assume that $\alpha \geq \beta$.

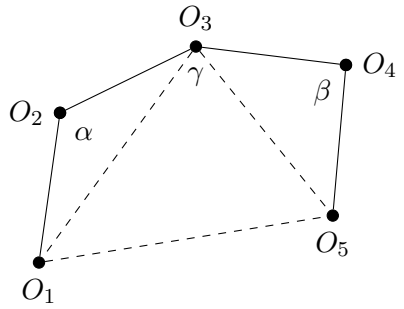

Figure 21. Interior angles of the path.

Then

$$\gamma = \theta - \left(\frac{\pi}{2} - \frac{\alpha}{2}\right) - \left(\frac{\pi}{2} - \frac{\beta}{2}\right) = \theta + \frac{\alpha+\beta}{2} - \pi.$$

First, observe that if $\alpha + \beta \geq \frac{5\pi}{3}$ or $\alpha - \beta \geq \frac{\pi}{3}$, then we are done. Indeed, if the former is true, then

$$\gamma = \theta + \frac{\alpha+\beta}{2} - \pi > \frac{\pi}{3} + \frac{5\pi}{6} - \pi = \frac{\pi}{6},$$

and if the latter is true, then

$$\gamma = \theta + \frac{\alpha+\beta}{2} - \pi > (\pi - \beta) + \frac{\alpha+\beta}{2} - \pi = \frac{\alpha-\beta}{2} \geq \frac{\pi}{6}.$$

Thus we may assume that $\alpha + \beta < \frac{5\pi}{3}$ and $\alpha - \beta < \frac{\pi}{3}$. We also know that $\frac{\pi}{3} < \beta \leq \alpha < \pi$.

Now, observe that $O_3O_1 = 4\sin\left(\frac{\alpha}{2}\right)$ and $O_3O_5 = 4\sin\left(\frac{\beta}{2}\right)$ by the Law of Cosines. Now, the Law of Cosines on $\triangle O_1O_3O_5$ gives that

$$(O_1O_5)^2 = 16\sin^2\left(\frac{\alpha}{2}\right) + 16\sin^2\left(\frac{\beta}{2}\right) - 32\sin\left(\frac{\alpha}{2}\right)\sin\left(\frac{\beta}{2}\right)\cos(\gamma).$$

Since $O_1O_5 > 2$, this implies that

$$\cos(\gamma) < \frac{\sin^2\left(\frac{\alpha}{2}\right) + \sin^2\left(\frac{\beta}{2}\right) - \frac{1}{4}}{2\sin\left(\frac{\alpha}{2}\right)\sin\left(\frac{\beta}{2}\right)}.$$

Verify the identity

$$\sin^2\left(\frac{\alpha}{2}\right) + \sin^2\left(\frac{\beta}{2}\right) - \frac{1}{4} - \sqrt{3}\cdot\sin\left(\frac{\alpha}{2}\right)\sin\left(\frac{\beta}{2}\right) = \left(\frac{\sqrt{3}}{2} + \cos\left(\frac{\alpha+\beta}{2}\right)\right)\left(\frac{\sqrt{3}}{2} - \cos\left(\frac{\alpha-\beta}{2}\right)\right)$$

by applying standard trigonometric identities. Since $0 < \alpha + \beta < \frac{5\pi}{3}$ and $0 \leq \alpha - \beta < \frac{\pi}{3}$, the product on the right side is greater than 0. Then the identity and inequality imply that

$$\frac{\sin^2\left(\frac{\alpha}{2}\right) + \sin^2\left(\frac{\beta}{2}\right) - \frac{1}{4}}{2\sin\left(\frac{\alpha}{2}\right)\sin\left(\frac{\beta}{2}\right)} < \frac{\sqrt{3}}{2},$$

so $\cos(\gamma) < \frac{\sqrt{3}}{2}$. This implies that $\gamma > \frac{\pi}{6}$ as desired. □

References

[1] David C. Brydges and John Z. Imbrie. Branched polymers and dimensional reduction. *Ann. of Math. (2)*, 158(3):1019–1039, 2003.

[2] L. Fejes Tóth. *Lagerungen in der Ebene, auf der Kugel und im Raum.* Die Grundlehren der Mathematischen Wissenschaften in Einzeldarstellungen mit besonderer Berücksichtigung der Anwendungsgebiete, Band LXV. Springer-Verlag, Berlin-Göttingen-Heidelberg, 1953.

[3] M. Fekete. Über die Verteilung der Wurzeln bei gewissen algebraischen Gleichungen mit ganzzahligen Koeffizienten. *Math. Z.*, 17(1):228–249, 1923.

[4] Ron Graham. Sets of points with given minimum separation (Solution to Problem E1921). *Amer. Math. Monthly*, 75(2):192–193, 1968.

[5] Helmut Groemer. Über die Einlagerung von Kreisen in einen konvexen Bereich. *Math. Z*, 73:285–294, 1960.

[6] J. M. Hammersley and K. W. Morton. Poor man's Monte Carlo. *J. Roy. Statist. Soc. Ser. B*, 16:23–38; discussion 61–75, 1954.

[7] Iwan Jensen. Improved lower bounds on the connective constants for two-dimensional self-avoiding walks. *J. Phys. A*, 37(48):11521–11529, 2004.

[8] Richard Kenyon and Peter Winkler. Branched polymers. *Amer. Math. Monthly*, 116(7):612–628, 2009.